

Structural and Functional Abnormalities in Children with Attention-Deficit/Hyperactivity Disorder: A Focus on Subgenual Anterior Cingulate Cortex

Chenyang Zhan,¹ Yuhong Liu,² Kai Wu,³ Yu Gao,⁴ and Xiaobo Li⁵⁻⁷

Abstract

Attention-deficit/hyperactivity disorder (ADHD), characterized by developmentally inappropriate inattention, hyperactivity/impulsivity, or a combination of both, is a major public health problem. Neuroimaging studies have revealed associations of these cognitive impairments with structural and functional deficits all over the brain. Existing findings are not fully consistent because of the heterogeneity of study samples and diversity of research techniques. In this study, we propose to utilize a multimodal magnetic resonance imaging (MRI) approach to study the structural and functional brain networks in children with ADHD-combined type (ADHD-C) with a focus on the subgenual anterior cingulate cortex (sgACC). Diffusion tensor imaging (DTI) and resting-state functional MRI (rs-fMRI) data from 32 children with ADHD-C and 32 group-matched controls were involved. Network-based statistic analysis of the rs-fMRI data revealed a disconnected functional network between the sgACC and multiple regions in the occipital lobe and cerebellum, whereas the DTI data showed disrupted white matter integrity in the subgenual cingulum bundle (sgCB). *Post hoc* region of interest (ROI)-based analyses showed significantly increased fluctuation of the spontaneous brain activity in the sgACC and higher radial diffusivity in the sgCB in the ADHD group. Both the rs-fMRI and DTI ROI-based measures were significantly correlated with clinical measures that examine behavioral capacities of attention and inhibitory control. Findings of this study suggest that functional alterations in the sgACC and white matter under development in the sgCB may impact each other, and together contribute to impaired attention and inhibitory control function in children with ADHD.

Keywords: ADHD; DTI; resting-state fMRI; subgenual anterior cingulate cortex; subgenual cingulum bundle

Introduction

ATENTION DEFICIT/HYPERACTIVITY DISORDER (ADHD) is the most prevalent neurodevelopmental disorder, characterized by developmentally inappropriate inattention, hyperactivity/impulsivity, or a combination of both (Pastor and Reuben, 2008). Currently, diagnosis of ADHD is relied on a questionnaire- and subjective observation-based model (Kupfer, 2000). A significant proportion of the children with ADHD also have anxiety and/or depression and other psychiatric comorbidities, many of whom later develop into clinically

diagnosed anxiety and/or major depression disorder (MDD) during adolescence or early adulthood (Inci et al., 2016). Understanding the neurobiological bases of this disorder is highly expected for the development of neurobiological criteria-based diagnosis model for this very heterogeneous syndrome (Martin Fernandez-Mayoralas et al., 2010).

Magnetic resonance imaging (MRI) is a robust noninvasive technique to study the neurobiological mechanisms of the brain. Reduced total brain volume and possible delay in posterior to anterior cortical maturation in children with ADHD have been revealed by structural MRI (sMRI) studies (Shaw

¹Department of Radiology, Albert Einstein College of Medicine, Bronx, New York.

²Department of Mathematics and Computer Science, Philander Smith College, Little Rock, Arkansas.

³Department of Biomedical Engineering, School of Materials Science and Engineering, South China University of Technology, Guangzhou, China.

⁴Department of Psychology, Brooklyn College and the Graduate Center of the City University of New York, Brooklyn, New York.

⁵Departments of Biomedical Engineering and ⁶Electric and Computer Engineering, New Jersey Institute of Technology, Newark, New Jersey.

⁷Department of Psychiatry, Icahn School of Medicine at Mount Sinai, New York, New York.

et al., 2007). Many task-based functional MRI (fMRI) studies have reported functional impairment in the frontal-striatal circuits, which are associated with the impaired inhibitory processes and attention control in ADHD (Castellanos et al., 2006). Functional impairments in more diverse regions including the cortices, cerebellum, as well as subcortical regions, such as thalamus, and their associations with cognitive and behavioral deficits in attention and cognitive control domains, have also been reported in children with ADHD (Castellanos and Proal, 2012; Krain and Castellanos, 2006; Li et al., 2012). Recent resting-state fMRI (rs-fMRI) studies also identified reduced functional connectivity (FC), abnormal topological properties of the default-mode network, and functional alterations in more widespread cortical regions in children with ADHD (Castellanos et al., 2008; Cocchi et al., 2012; Liston et al., 2011; Wang et al., 2009). These findings suggest that multiple brain circuits are likely to be involved, and together contribute to the cognitive and behavioral dysfunctions in ADHD (Castellanos and Proal, 2012).

Compared with sMRI and fMRI, diffusion tensor imaging (DTI) is a relatively new MRI technique that studies the integrity of white matter structures (Ashtari et al., 2005). Because of the myelin sheath, water diffusion in axonal fibers exhibits an anisotropic feature, that is, the water diffusion is faster along the axial direction (parallel to the fiber) and slower in the radial direction (perpendicular to the fiber). DTI calculates the water diffusion vector in each voxel and quantifies diffusive values such as fractional anisotropy (FA), mean diffusivity (MD), axial diffusivity (L1), and radial diffusivity (RD) (Damoiseaux and Greicius, 2009; Zhu and Majumdar, 2012). Alterations of these values have been correlated with microstructural change in axonal fibers, as confirmed by histological studies in animals (Song et al., 2002, 2003). Reduced white matter structural integrity in the frontal-striatal tracts has been frequently observed in DTI studies in children with ADHD (van Ewijk et al., 2012), whereas abnormalities in the other brain regions including corpus callosum, cingulum bundle (CB), and cerebellum have also been reported (Ashtari et al., 2005; Liston et al., 2011; Makris et al., 2008; Pavuluri et al., 2009). Inconsistencies of structural and functional findings in ADHD studies are partly because of the intrinsic heterogeneity in the pathophysiology of ADHD (Liston et al., 2011), and methodological differences such as sample size, age range, clinical status (particularly ADHD subtypes and the medication status), and different MRI modalities been implemented (van Ewijk et al., 2012, 2014).

The majority of the existing neuroimaging studies in children with ADHD focused on understanding the neuronal substrates of inattention and hyperactive/impulsive components in the disorder. The neuronal underpinnings of the significant high risk for developing anxiety, depression, and other psychiatric symptoms, which also characterize the disorder, have not yet been well investigated. By the combination of sMRI and rs-fMRI analyses, Posner and associates found that structural and functional abnormalities associated with hippocampus may contribute to depressive symptoms in children with ADHD (Posner et al., 2014). We hypothesize that structural and/or functional anomalies in subgenual anterior cingulate cortex (sgACC), which plays a critical role in emotion regulation and has been found to contribute to MDD and other mood disorders (Drevets et al., 1997; Hir-

ayasu et al., 1999; Yucel et al., 2009), may associate with impulsivity in children with ADHD, and together serve as a vulnerable marker for developing MDD and other mood disorders. In this study, we proposed to use a multimodal MRI approach, including both rs-fMRI and DTI, to investigate our hypothesis.

Materials and Methods

Participants

A total of 70 children, aged from 9 to 15 years old, participated in this study. After excluding 6 participants because of heavy head motion in the MRI data, 32 children with ADHD and 32 controls were included in final fMRI and DTI data analyses. The ADHD participants were recruited based on the DSM-IV criteria for the ADHD-combined type. The controls were involved if the T scores <60 (<1 SD) on all the Conners parent and self-report ADHD subscales (ADHD-hyperactive, -inattentive, and total scores) (Conners, 2008). For both groups, we used the new schedule for affective disorders and schizophrenia for school-aged children screening questionnaire and supplements as appropriate to rule out pervasive developmental disorders, substance use and abuse, and post-traumatic stress (Kaufman et al., 1997). Oppositional defiant disorder with physical aggression and other Axis I disorders (except for fear of the dark) were exclusionary. Additional exclusion criteria for the whole study sample included histories of head trauma or seizures, MRI safety and artifact risk factors (e.g., teeth braces), or low IQ [below 80, measured by the Wechsler Abbreviated Scale of Intelligence-II (Wechsler, 1999)]. Up to the study date, none of the entire study cohort had clinically diagnosed anxiety, MDD, or other mood disorders.

The children with ADHD were recruited from the Children's Evaluation and Rehabilitation Center at the Albert Einstein College of Medicine, and the Max and Celia Parnes Family Psychological and Psychoeducational Services Clinic at the Ferkauf Graduate School of Psychology of Yeshiva University. The controls were recruited from local schools through newspaper advertisements. This study received Institutional Review Board Approval for human subjects' research at Albert Einstein College of Medicine of Yeshiva University. After the study and its procedures were carefully explained, all participants and their parents provided written informed consents.

MRI data acquisition

Imaging data were acquired using a 3.0 Tesla 32 Channel Free wave Achieva MRI Scanner (Philips Medical Systems, Best, The Netherlands). High-resolution T1-weighted sMRI images were scanned at 1 mm isotropic resolution (TR = 9.8 msec, TE = 4.6 msec, flip angle = 8°, field of view [FOV] = 240 mm × pt? > 188 mm × 220 mm). The 6-min duration rs-fMRI data were acquired using echo-planar imaging (EPI) sequence (TE = 28 msec, TR = 2000 msec, 2 mm isotropic resolution, 230 mm FOV, imaging matrix = 230 × 128, number of slices = 49). DTI acquisition used EPI sequence with a b-value of 800 sec/mm² along 32 independent, noncollinear orientations (TR = 7367 msec, TE = 56 msec, 2 mm isotropic resolution, FOV = 240 mm × 249 mm, imaging matrix = 144 × 144, number of slices = 70, SENSE factor = 2.5). A nondiffusion weighted image (b0 image) was also collected.

rs-fMRI data preprocessing

The rs-fMRI data from each participant were preprocessed using the FSL/FEAT tools (Smith et al., 2004). Each rs-fMRI imaging data set was initially corrected for slice timing, spatial intensity, and spatially smoothed with a 4 mm full-width and half maximum Gaussian kernel. For head motion analyses, traditional measurement of the six translation and rotation parameters was first calculated from the rigid body transformation for head realignment. In addition, head motion effects in the blood oxygen-level dependent (BOLD) signals and their putative effects on FC patterns in the fMRI data were assessed by using the frame-wise measurements of the six realignment parameters (Li et al., 2013; Power et al., 2012). Finally, a band pass temporal filter of 0.01–0.1 Hz was applied. Nonbrain structures were extracted. The fMRI data were first aligned to the skull-stripped T1-weighted image from the same participant using an affine translation and further registered to the MNI152 template. The voxel-based whole brain β map was created using linear regression with a model of “constant on.” Nine motion components in the time series were added as covariates in the multiple linear regression model. Each of the 90 cortical and subcortical regions defined in the automated anatomical labeling (AAL) atlas was selected as a region of interest (ROI) (Tzourio-Mazoyer et al., 2002). Pearson correlation of the average time series in each pair of the AAL atlas-based ROIs was calculated. Two FC matrices were constructed in each brain by using the absolute versus positive-only values of the correlation coefficients.

Network-based statistics analysis

The network-based statistics (NBS) seeks to identify any potentially connected regions formed by an appropriately chosen set of suprathreshold links (Zalesky et al., 2010). The topological extent of any such region is then used to determine its significance. For each participant, the FC matrix, constructed based on the $(90 \times 89)/2 = 4005$ pairs of ROIs, was the input of this analysis. A between-group t test of the absolute Pearson correlation coefficient of each pair of the regions was calculated. This step was repeated independently in the 4005 pairs of ROIs. Pairs of regions, which had a t statistic exceeding a threshold 3.8 (uncorrected $p < 0.01$), were systematically searched as potential components for any interconnected networks that might have between-group difference (Cocchi et al., 2012). Meanwhile, the connected nodes, which might present in the set of suprathreshold links, were identified by using breadth-first search. Then a family-wise error (FWE)-corrected p value was then ascribed to each interconnected network by running the permutation test. For each permutation, the subjects were randomly exchanged between the ADHD and the control groups. The NBS was then applied to the randomized data, and the size of the largest interconnected network was recorded. In our study, a total of 10,000 permutations were generated to yield an empirical null distribution for the size of the largest interconnected network. As the final step, the corrected p value for an interconnected network of size k was calculated as the proportion of the permutations for which the largest network was greater than or equal to k . As a result, we demonstrated the interconnected networks that had an FWE-corrected value of $p < 0.05$.

Based on the result provided by NBS analyses, a spherical ROI from the left side sgACC (origin $[-9, 15, -12]$, radius

$R = 4$ mm) was generated. The average t value among all the voxels within this ROI was calculated in each datum to represent the mean magnitude of spontaneous brain activity in this ROI (the higher the average t , the lower the fluctuation).

DTI analysis

DTI data were preprocessed using FSL/Diffusion Toolbox (Behrens et al., 2007; Xia et al., 2012). After eddy current correction and brain extraction, the diffusion-weighted images for each subject were registered to the additionally acquired nondiffusion-weighted reference image (b0 image) using an affine, 12 degrees of freedom registration (Jenkinson and Smith, 2001). Then the values for FA, L1, and RD at each brain voxel were computed. The FA images were scaled, automatically aligned to the most typical subject in the study, and registered to the standard space using tract-based spatial statistics (TBSS) (Smith et al., 2006). The nonlinear warps for FA images were then applied to L1 and RD images for registration.

Based on results of the TBSS analysis, two spherical ROIs (radius 3 mm) were generated in subgenual cingulum bundle (sgCB) with origin of $[-7, 41, 3]$, and premotor cortex (PMC) of $[38, -1, 31]$. The MD values in each ROI were extracted.

Group statistics

Group differences of the demographic and clinical measures were examined using t and χ^2 tests.

For the rs-fMRI data, the NBS technique itself provided the result of between-group comparison with an FWE-corrected value of $p < 0.05$. For the DTI data, group statistical analysis was conducted only on voxels within the white matter skeleton mask. Between-group differences of FA, MD, and RD values were assessed using voxel-wise two-sample t tests. Nonparametric permutation tests and threshold-free cluster enhancement (TFCE) option were conducted based on 5000 random permutations. The clusters with a TFCE-corrected p value of less than 0.05 or 0.0001 were reported.

Pearson correlation analyses were carried out between the ROI-based imaging outcome measures (BOLD activation in sgACC, and white matter measures in sgCB and PMC) and the clinical scores for assessing inattentiveness and hyperactivity/impulsivity (DSM-IV inattentive, hyperactive, and total scores), by controlling the potential confounding effects because of IQ, age, and gender. Multiple comparisons were corrected for the correlation analyses by using the false discovery rate (FDR) approach at $\alpha = 0.05$, and a significance threshold of $p < 0.05$.

Results

The demographic and clinical data of the participants in this study are described in Table 1. The ADHD and control groups did not significantly differ in age, gender, and full scale IQ.

The correlation coefficient absolute value-based NBS analysis of the rs-fMRI data showed one network of significantly decreased connectivity in the ADHD group ($p_{\text{FWE}} = 0.035$) (Fig. 1). Remarkably, the left side sgACC formed the hub of this disconnected network, which was connected to six other nodes in bilateral occipital lobes (left cuneus, superior occipital gyri; right cuneus, calcarine, and lingual

TABLE 1. DEMOGRAPHIC AND CLINICAL CHARACTERISTICS OF THE PARTICIPANTS

	Controls (N=32) (mean ± SD)	ADHD (N=32) (mean ± SD)	Test statistic	p
Age	11.9 ± 0.4	11.1 ± 0.3	$t = 1.78$	0.081
Male/female	19/13	25/7	$\chi^2 = 2.62$	0.106
Full-scale IQ	108.1 ± 2.3	104.3 ± 2.4	$t = 1.14$	0.259
P inattent T	46.7 ± 1.0	66.8 ± 1.6	$t = 10.64$	<0.001
P hyp. imp. T	48.6 ± 1.7	71.8 ± 2.3	$t = 8.15$	<0.001
P DSM-IV T	47.7 ± 1.3	70.7 ± 1.8	$t = 10.22$	<0.001

P DSM-IV T, T score for sum of total raw scores; P inattent T, parent inattentive T score; P hyp. imp. T, parent hyperactive-impulsive T score.

gyri) and left cerebellum lobule VI. The right side sgACC was also found to be significantly disconnected with bilateral cerebellum lobule VI. However, the positive correlation coefficient value-based NBS analysis showed significantly decreased connectivity in an inner network including the left side sgACC connected to five other nodes in bilateral occipital lobes (left cuneus, superior occipital gyri; right cuneus, calcarine, and lingual gyri).

ROI-based analysis in rs-fMRI data showed a trend of increased fluctuation of the spontaneous brain activation in the left sgACC region ($t = 1.80$, $p = 0.08$) in the ADHD group, when compared with the controls.

Group comparisons in the DTI data revealed two clusters of significantly elevated RD in the ADHD group, one at sgCB and the other in PMC (Fig. 2). *Post hoc* ROI-based analyses showed that the mean RD values in both sgCB and PMC ROIs were significantly higher in the ADHD group (in sgCB, the mean RD was $[0.83 \pm 0.01] \times 10^{-3}$ mm²/sec in ADHD group, and $[0.76 \pm 0.01] \times 10^{-3}$ mm²/sec in control group ($t = 4.32$, $p < 0.001$); whereas in PMC, the mean RD was $[0.78 \pm 0.01] \times 10^{-3}$ mm²/sec in ADHD group, and $[0.69 \pm 0.02] \times 10^{-3}$ mm²/sec in control group [$t = 4.60$, $p < 0.001$]). No significant between-group differences were reported in FA and MD measures.

In the ADHD group, the mean BOLD signal of the sgACC ROI exhibited a negative correlation with the DSM-hyperactive index ($R = -0.52$, $p = 0.0026$), and the DSM-

total index ($R = -0.36$, $p = 0.046$) (Fig. 3). In the whole study sample, RD in both sgCB and PMC demonstrated significant (or a trend of significance) positive correlations with the clinical scores (Fig. 4A–F).

Discussion

sgACC dysfunctions in children with ADHD

NBS-based analysis of the rs-fMRI data identified a significantly disconnected functional network in the ADHD group, with the left sgACC being the only dominant hub of the disconnectivity (Fig. 1). sgACC is located below genu of the Corpus Callosum. Previous neuroimaging studies have reported that this region plays a critical role in emotion regulation. A decrease of gray matter volume in sgACC has been found in patients with bipolar disorder (Drevets et al., 1997; Hirayasu et al., 1999) and MDD (Yucel et al., 2009). In adolescents with MDD, the nerve fibers arising from the sgACC have been found to have lower FA (Cullen et al., 2010). Suicidal patients with impulsivity and depression (more than half of these patients had ADHD) exhibited decreased cerebral blood flow in the sgACC (Willeumier et al., 2011). Recently, altered resting-state FC between the sgACC and several cortical regions was reported in adolescents with MDD (Connolly et al., 2013), which was consistent with our findings. Our findings also demonstrated that the BOLD signals in the left

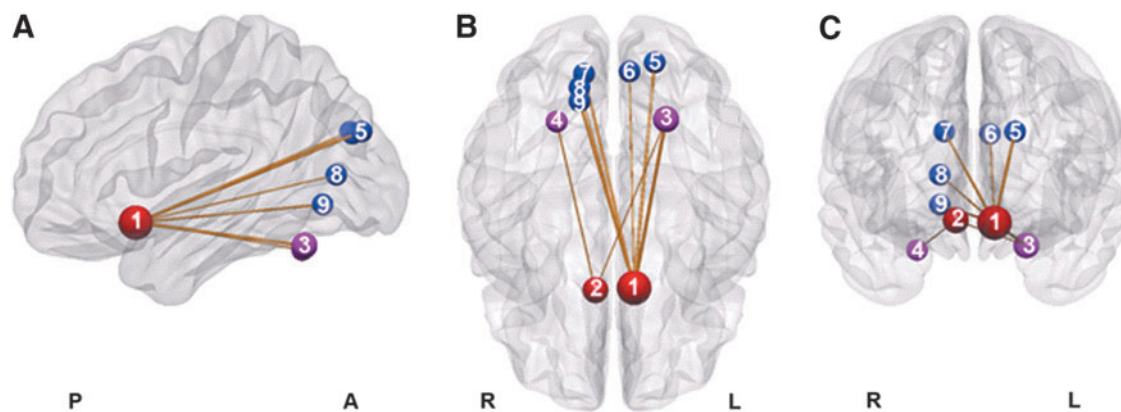


FIG. 1. A disconnected functional network in ADHD revealed by the network-based statistics analysis in resting-state fMRI data (nodes of the disconnected network are represented by spheres in sagittal (A), axial (B), and coronal (C) views. Regions in the sgACC, occipital lobe, and cerebellum are in red, blue, and magenta, respectively. 1, left sgACC; 2, right sgACC; 3, left cerebellum lobule VI; 4, right cerebellum lobule VI; 5, left superior occipital gyrus; 6, left cuneus gyrus; 7, right cuneus gyrus; 8, right calcarine gyrus; 9, right lingual gyrus). ADHD, attention-deficit/hyperactivity disorder; fMRI, functional magnetic resonance imaging; sgACC, subgenual anterior cingulate cortex. Color images available online at www.liebertpub.com/brain

FIG. 2. White matter abnormalities in ADHD (RD was significantly increased in the sgCB (red in **A**) and PMC (red in **B**) in the ADHD group). For demonstration, the sgCC (Fig. 1) is displayed as a blue spot in (**A**). PMC, premotor cortex; RD, radial diffusivity; sgCB, subgenual cingulum bundle; sgCC, subgenual cingulate cortex. Color images available online at www.liebertpub.com/brain

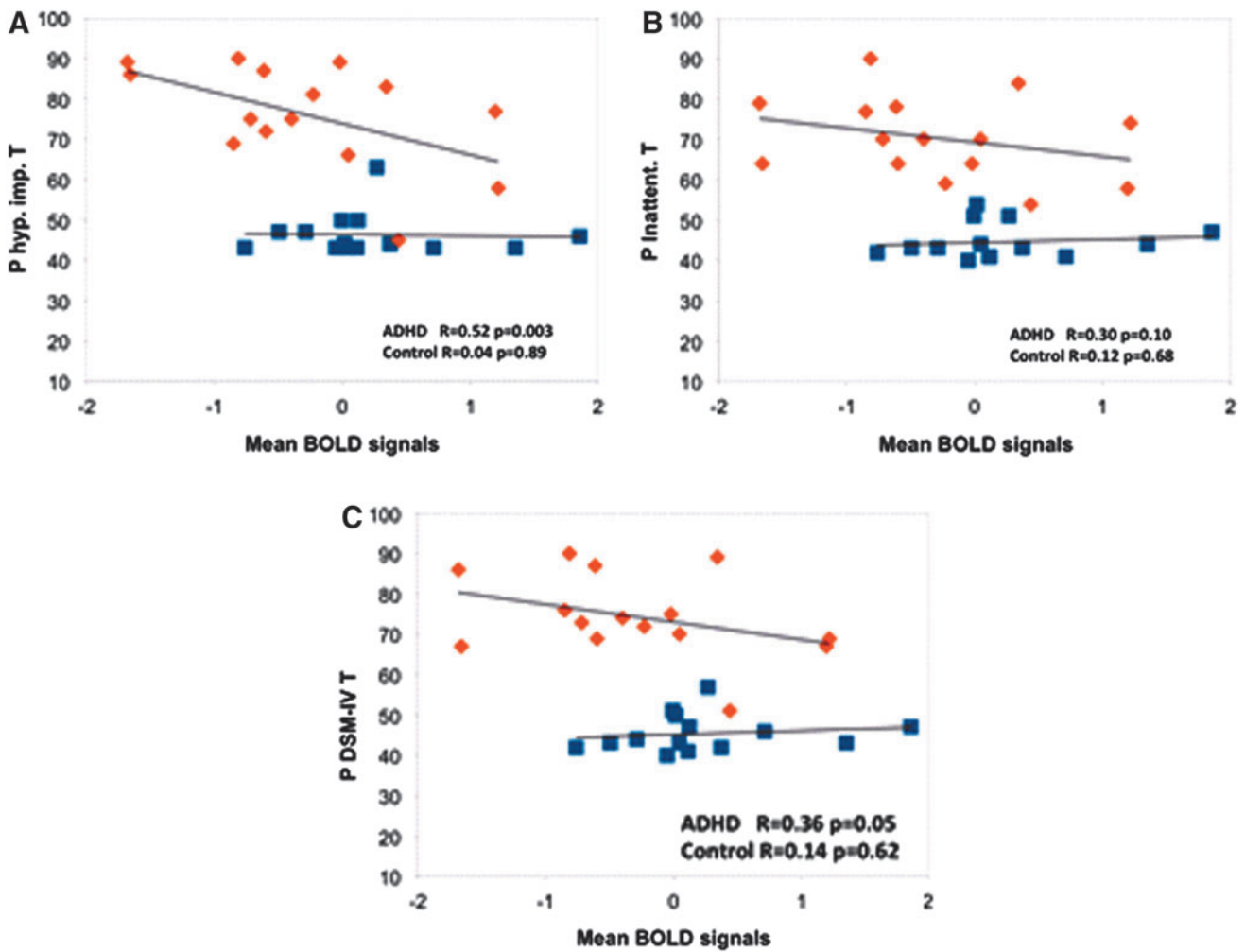
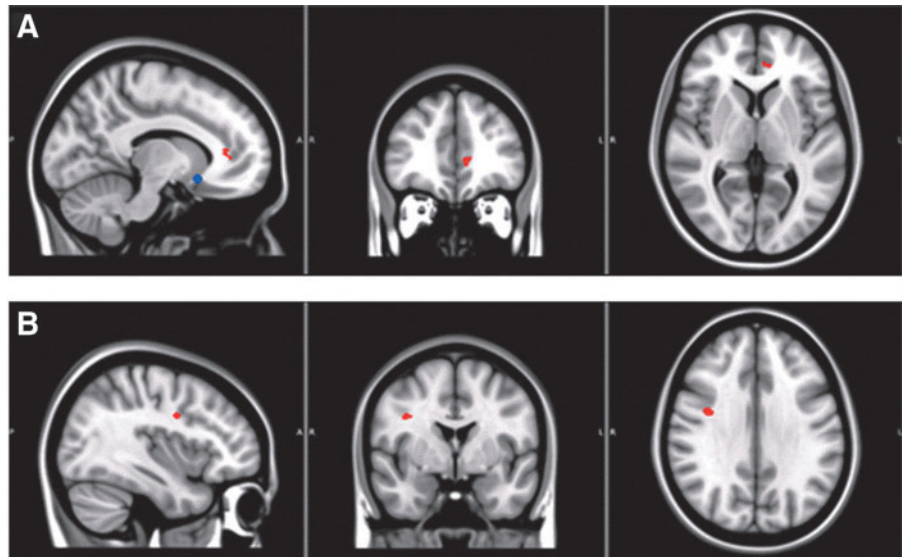


FIG. 3. Increased fluctuation of the spontaneous functional activation in the left sgACC was significantly correlated with increased clinical symptom severity in ADHD (average t value of a spherical ROI in sgACC was plotted with the parent hyperactive-impulsive T score (**A**), parent inattentive T score (**B**), and T score for sum of total raw scores (**C**). ADHD patients and normal controls are represented by orange diamonds (\blacklozenge) and blue squares (\blacksquare), respectively. ROI, region of interest. Color images available online at www.liebertpub.com/brain

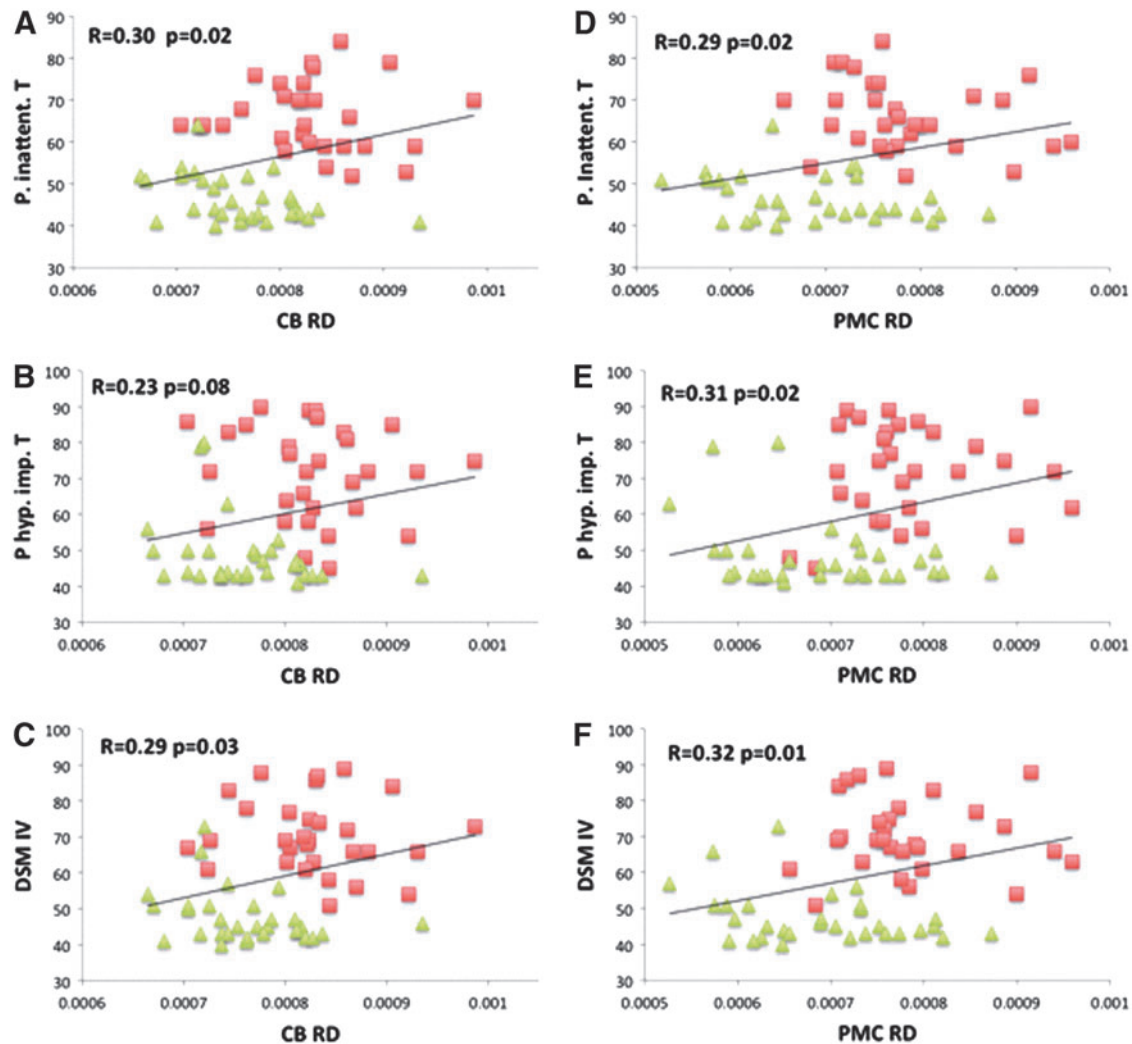


FIG. 4. Increased RD in sgCB and PMC was significantly correlated with the ADHD-associated symptom severity scores in the whole study sample (the average RD of the spherical ROIs in sgCB (A–C) and PMC (D–F) is plotted with the parent inattentive T score (A, D), parent hyperactive-impulsive T score (B, E), and T score for sum of total raw scores (C, F). The ADHD patients and normal controls are represented by red square (■) and green triangle (▲), respectively. Correlation coefficient (R) and p value for each correlation analysis are displayed in the subplot. Color images available online at www.liebertpub.com/brain

sgACC were negatively correlated with DSM-impulsivity scores in the ADHD group, but not in controls (Fig. 3), whereas the correlation between the BOLD signal and DSM-inattention score was not highly significant in the ADHD group ($p=0.10$).

Compared with the general population, children with ADHD have a heightened risk for developing MDD and other mood disorders (Daviss, 2008). Taken together, findings suggest that decreased spontaneous brain activity in the sgACC and its disconnectivity with other brain regions contribute to the impulsivity component in children with ADHD, and may suggest comorbidity or later onset of depressive symptoms in the affected individuals.

sgACC-involved dysfunctional brain network in children with ADHD

The NBS-based analysis demonstrated that the left sgACC is functionally disconnected with five regions in the occipital

cortex in the ADHD group. Two of the five disconnected regions are ipsilateral (left cuneus gyrus and superior occipital gyrus), and the other three are contralateral (right cuneus gyrus, calcarine gyrus, and lingual gyrus). To our knowledge, this is the first report of functional disconnections between the sgACC and the occipital lobe in children with ADHD. The occipital cortex is essential in the regulation of visual attentional network (Castellanos and Proal, 2012). sMRI and fMRI studies have reported reduced gray matter volume in medial occipital lobe (Proal et al., 2011), and decreased nodal efficiency of lingual gyrus and calcarine cortex in the resting-state functional brain network in children with ADHD (Wang et al., 2009). More recently, by using rsfMRI and NBS, Cocchi and associates reported enhanced FC of the lingual and superior occipital cortices with orbitofrontal and temporal cortices, respectively, in young adults with ADHD (Cocchi et al., 2012). In our results, regions all over the occipital cortex were significantly disconnected with left sgACC, whereas no regions from the

orbitofrontal or temporal cortices were involved. Differences among these findings may reflect the complex nature, population heterogeneity, and neurodevelopmental diversity in children with ADHD.

Besides the occipital cortex, cerebellum also showed decreased connectivity with sgACC in children with ADHD. The cerebellum controls motor movement, and is engaged in emotional and cognitive functions (Krain and Castellanos, 2006; Stoodley et al., 2012). Smaller cerebellar volume in children with ADHD has been reported, mainly lying in lobules VIII to X (Krain and Castellanos, 2006). Our fMRI data demonstrated functional disconnectivity of the right hemisphere sgACC with left lobule VI in the ADHD group (Fig. 1). Lobule VI is located between the primary and superior posterior fissures. This lobule can be activated by negative emotions (Schraa-Tam et al., 2012), and is engaged in cognitive tasks such as verb generation and working memory task (Stoodley et al., 2012).

White matter microstructural underdevelopment in children with ADHD

Our DTI data analyses revealed significantly higher RD in the left sgCB and right PMC in children with ADHD, which reflect the reduced white matter integrity in these regions. L1 is the principal eigenvalue, and RD is the average of the second and third eigenvalues of the ellipsoidal function. Therefore, by definition, L1 and RD are parallel and perpendicular to the diffusion direction, respectively. Increase of RD coupled with unchanged L1 has been suggested to be a possible sign of demyelination (Song et al., 2002).

CB is a longitudinal white matter tract between corpus callosum and cingulate gyrus. It extends from genu of the corpus callosum rostrally to splenium caudally, and includes both long- and short-range fibers connecting the limbic system (Yakovlev and Locke, 1961) and multiple cortical and subcortical regions in the prefrontal, parietal, and temporal lobes (Jones et al., 2013). sgCB is the anterior part of the CB and is located underneath the sgACC. The fibers of this tract connect multiple regions of the ACC, as well as other regions such as diagonal band and medial septum (Jones et al., 2013). Voxel-wise analysis of DTI data revealed decreased FA in the sgCB in adolescents with MDD (Cullen et al., 2010) and in adults with ADHD (Makris et al., 2008). Our result of increased RD in the sgCB is consistent with findings from these previous studies, and suggests that disrupted white matter microstructure in the sgCB may be a persistent structural marker in children and adults with ADHD.

Limitations

A few limitations may apply to this work. First, both female and male participants were involved in this study. Clinical symptoms of ADHD have been shown to be different between male and female patients (Biederman et al., 2002). Owing to the insufficient female sample in the ADHD group, we could not conduct between-gender comparisons in this study. Herein, gender was included as a covariate in the main analyses of both fMRI and DTI data to reduce the gender-related effect to the study results. Further group-level assessments of both fMRI and DTI data in only male subjects (19 controls and 25 patients) did not show sig-

nificant differences from the main findings. Second, 9 of the 32 children with ADHD had been taking short-acting medications, whereas the others were medication naive. However, we requested a minimum of a 48-h wash-out period before MRI data acquisition to eliminate the medication effects on brain activations. Impact of the short-acting stimulant medications on brain structures has not been observed in ADHD studies.

Conclusions

In this study, a combination of functional and diffusional MRI techniques was utilized to investigate the functional and structural brain alterations in children with ADHD. NBS analysis of the rs-fMRI data revealed a disconnected functional network between the sgACC and multiple regions in the occipital lobe and cerebellum, whereas the DTI data showed disrupted white matter integrity in the sgCB. *Post hoc* ROI-based analyses showed significantly reduced spontaneous brain activity in the sgACC and significantly higher RD in the sgCB in the ADHD group. These fMRI and DTI ROI-based measures are significantly correlated with clinical measures that examine behavioral capacities of attention or inhibitory control.

Acknowledgments

This work was partially supported by NIMH (R03MH109791), NICHD (HD071593), and the NJIT Faculty Seed Award to Dr. Xiaobo Li.

Author Disclosure Statement

No competing financial interests exist.

References

- Ashtari M, Kumra S, Bhaskar SL, Clarke T, Thaden E, Cervellione KL, et al. 2005. Attention-deficit/hyperactivity disorder: a preliminary diffusion tensor imaging study. *Biol Psychiatry* 57:448–455.
- Behrens TE, Berg HJ, Jbabdi S, Rushworth MF, Woolrich MW. 2007. Probabilistic diffusion tractography with multiple fibre orientations: what can we gain? *Neuroimage* 34:144–155.
- Biederman J, Mick E, Faraone SV, Braaten E, Doyle A, Spencer T, et al. 2002. Influence of gender on attention deficit hyperactivity disorder in children referred to a psychiatric clinic. *Am J Psychiatry* 159:36–42.
- Castellanos FX, Margulies DS, Kelly C, Uddin LQ, Ghaffari M, Kirsch A, et al. 2008. Cingulate-precuneus interactions: a new locus of dysfunction in adult attention-deficit/hyperactivity disorder. *Biol Psychiatry* 63:332–337.
- Castellanos FX, Proal E. 2012. Large-scale brain systems in ADHD: beyond the prefrontal-striatal model. *Trends Cogn Sci* 16:17–26.
- Castellanos FX, Sonuga-Barke EJ, Milham MP, Tannock R. 2006. Characterizing cognition in ADHD: beyond executive dysfunction. *Trends Cogn Sci* 10:117–123.
- Cocchi L, Bramati IE, Zalesky A, Furukawa E, Fontenelle LF, Moll J, et al. 2012. Altered functional brain connectivity in a non-clinical sample of young adults with attention-deficit/hyperactivity disorder. *J Neurosci* 32:17753–17761.
- Conners CK. 2008. *Conners*. 3rd ed. Toronto: Multi-Health Systems, Inc.
- Connolly CG, Wu J, Ho TC, Hoeft F, Wolkowitz O, Eisendrath S, et al. 2013. Resting-state functional connectivity of

- subgenual anterior cingulate cortex in depressed adolescents. *Biol Psychiatry* 74:898–907.
- Cullen KR, Klimes-Dougan B, Muetzel R, Mueller BA, Camchong J, Houry A, et al. 2010. Altered white matter microstructure in adolescents with major depression: a preliminary study. *J Am Acad Child Adolesc Psychiatry* 49:173–183 e171.
- Damoiseaux JS, Greicius MD. 2009. Greater than the sum of its parts: a review of studies combining structural connectivity and resting-state functional connectivity. *Brain Struct Funct* 213:525–533.
- Daviss WB. 2008. A review of co-morbid depression in pediatric ADHD: etiology, phenomenology, and treatment. *J Child Adolesc Psychopharmacol* 18:565–571.
- Drevets WC, Price JL, Simpson JR, Jr., Todd RD, Reich T, Vanier M, et al. 1997. Subgenual prefrontal cortex abnormalities in mood disorders. *Nature* 386:824–827.
- Hirayasu Y, Shenton ME, Salisbury DF, Kwon JS, Wible CG, Fischer IA, et al. 1999. Subgenual cingulate cortex volume in first-episode psychosis. *Am J Psychiatry* 156:1091–1093.
- Inci SB, Ipci M, Akyol Ardic U, Ercan ES. 2016. Psychiatric comorbidity and demographic characteristics of 1,000 children and adolescents with ADHD in Turkey. *J Atten Disord* [Epub ahead of print] DOI: 10.1177/1087054716666954.
- Jenkinson M, Smith S. 2001. A global optimisation method for robust affine registration of brain images. *Med Image Anal* 5:143–156.
- Jones DK, Christiansen KF, Chapman RJ, Aggleton JP. 2013. Distinct subdivisions of the cingulum bundle revealed by diffusion MRI fibre tracking: implications for neuropsychological investigations. *Neuropsychologia* 51:67–78.
- Kaufman J, Birmaher B, Brent D, Rao U, Flynn C, Moreci P, et al. 1997. Schedule for Affective Disorders and Schizophrenia for School-Age Children-Present and Lifetime Version (K-SADS-PL): initial reliability and validity data. *J Am Acad Child Adolesc Psychiatry* 36:980–988.
- Krain AL, Castellanos FX. 2006. Brain development and ADHD. *Clin Psychol Rev* 26:433–444.
- Kupfer DJ. 2000. National Institutes of Health Consensus Development Conference Statement: diagnosis and treatment of attention-deficit/hyperactivity disorder (ADHD). *J Am Acad Child Adolesc Psychiatry*, 39:182–193.
- Li X, Branch C, De La Fuente A, Xia S. 2013. Role of pulvinar-cortical functional brain pathways in attention-deficit/hyperactivity disorder. *J Am Acad Child Adolesc Psychiatry* 52:756–758.
- Li X, Srubek A, Kelly MS, Lesser I, Sussman E, He Y, et al. 2012. Atypical pulvinar-cortical pathways during sustained attention performance in children with attention-deficit/hyperactivity disorder. *J Am Acad Child Adolesc Psychiatry* 51:1197–1207 e1194.
- Liston C, Malter Cohen M, Teslovich T, Levenson D, Casey BJ. 2011. Atypical prefrontal connectivity in attention-deficit/hyperactivity disorder: pathway to disease or pathological end point? *Biol Psychiatry* 69:1168–1177.
- Makris N, Buka SL, Biederman J, Papadimitriou GM, Hodge SM, Valera EM, et al. 2008. Attention and executive systems abnormalities in adults with childhood ADHD: A DT-MRI study of connections. *Cereb Cortex* 18:1210–1220.
- Martin Fernandez-Mayoralas D, Fernandez-Jaen A, Garcia-Segura JM, Quinones-Tapia D. 2010. [Neuroimaging in attention deficit hyperactivity disorder]. *Rev Neurol* 50 Suppl 3:S125–133.
- Pastor PN, Reuben CA. 2008. Diagnosed attention deficit hyperactivity disorder and learning disability: United States, 2004–2006. *Vital Health Stat* 10:1–14.
- Pavuluri MN, Yang S, Kamineni K, Passarotti AM, Srinivasan G, Harral EM, et al. 2009. Diffusion tensor imaging study of white matter fiber tracts in pediatric bipolar disorder and attention-deficit/hyperactivity disorder. *Biol Psychiatry* 65:586–593.
- Posner J, Siciliano F, Wang Z, Liu J, Sonuga-Barke E, Greenhill L. 2014. A multimodal MRI study of the hippocampus in medication-naïve children with ADHD: what connects ADHD and depression? *Psychiatry Res* 224:12–118.
- Power JD, Barnes KA, Snyder AZ, Schlaggar BL, Petersen SE. 2012. Spurious but systematic correlations in functional connectivity MRI networks arise from subject motion. *Neuroimage* 59:2142–2154.
- Proal E, Reiss PT, Klein RG, Mannuzza S, Gotimer K, Ramos-Olagastí MA, et al. 2011. Brain gray matter deficits at 33-year follow-up in adults with attention-deficit/hyperactivity disorder established in childhood. *Arch Gen Psychiatry* 68:1122–1134.
- Schraa-Tam CK, Rietdijk WJ, Verbeke WJ, Dietvorst RC, van den Berg WE, Bagozzi RP, et al. 2012. fMRI activities in the emotional cerebellum: a preference for negative stimuli and goal-directed behavior. *Cerebellum* 11:233–245.
- Shaw P, Eckstrand K, Sharp W, Blumenthal J, Lerch JP, Greenstein D, et al. 2007. Attention-deficit/hyperactivity disorder is characterized by a delay in cortical maturation. *Proc Natl Acad Sci U S A* 104:19649–19654.
- Smith SM, Jenkinson M, Johansen-Berg H, Rueckert D, Nichols TE, Mackay CE, et al. 2006. Tract-based spatial statistics: voxelwise analysis of multi-subject diffusion data. *Neuroimage* 31:1487–1505.
- Smith SM, Jenkinson M, Woolrich MW, Beckmann CF, Behrens TE, Johansen-Berg H, et al. 2004. Advances in functional and structural MR image analysis and implementation as FSL. *Neuroimage* 23 Suppl 1:S208–219.
- Song SK, Sun SW, Ju WK, Lin SJ, Cross AH, Neufeld AH. 2003. Diffusion tensor imaging detects and differentiates axon and myelin degeneration in mouse optic nerve after retinal ischemia. *Neuroimage* 20:1714–1722.
- Song SK, Sun SW, Ramsbottom MJ, Chang C, Russell J, Cross AH. 2002. Dysmyelination revealed through MRI as increased radial (but unchanged axial) diffusion of water. *Neuroimage* 17:1429–1436.
- Stoodley CJ, Valera EM, Schmahmann JD. 2012. Functional topography of the cerebellum for motor and cognitive tasks: an fMRI study. *Neuroimage*, 59:1560–1570.
- Tzourio-Mazoyer N, Landeau B, Papathanassiou D, Crivello F, Etard O, Delcroix N, et al. 2002. Automated anatomical labeling of activations in SPM using a macroscopic anatomical parcellation of the MNI MRI single-subject brain. *Neuroimage* 15:273–289.
- van Ewijk H, Heslenfeld DJ, Zwiers MP, Buitelaar JK, Oosterlaan J. 2012. Diffusion tensor imaging in attention deficit/hyperactivity disorder: a systematic review and meta-analysis. *Neurosci Biobehav Rev* 36:1093–1106.
- van Ewijk H, Heslenfeld DJ, Zwiers MP, Faraone SV, Luman M, Hartman CA, et al. 2014. Different mechanisms of white matter abnormalities in attention-deficit/hyperactivity disorder: a diffusion tensor imaging study. *J Am Acad Child Adolesc Psychiatry* 53:790–799 e793.
- Wang L, Zhu C, He Y, Zang Y, Cao Q, Zhang H, et al. 2009. Altered small-world brain functional networks in children

- with attention-deficit/hyperactivity disorder. *Hum Brain Mapp* 30:638–649.
- Wechsler D. 1999. *Wechsler Abbreviated Scale of Intelligence (WASI)*. San Antonio, TX: The Psychological Corporation.
- Willeumier K, Taylor DV, Amen DG. 2011. Decreased cerebral blood flow in the limbic and prefrontal cortex using SPECT imaging in a cohort of completed suicides. *Transl Psychiatry* 1:e28.
- Xia S, Li X, Kimball AE, Kelly MS, Lesser I, Branch C. 2012. Thalamic shape and connectivity abnormalities in children with attention-deficit/hyperactivity disorder. *Psychiatry Res* 204:161–167.
- Yakovlev PI, Locke S. 1961. Limbic nuclei of thalamus and connections of limbic cortex. III. Corticocortical connections of the anterior cingulate gyrus, the cingulum, and the subcallosal bundle in monkey. *Arch Neurol* 5:364–400.
- Yucel K, McKinnon M, Chahal R, Taylor V, Macdonald K, Joffe R, et al. 2009. Increased subgenual prefrontal cortex size in remitted patients with major depressive disorder. *Psychiatry Res* 173:71–76.
- Zalesky A, Fornito A, Bullmore ET. 2010. Network-based statistic: identifying differences in brain networks. *Neuroimage* 53:1197–1207.
- Zhu DC, Majumdar S. 2014. Integration of resting-state fMRI and diffusion-weighted MRI connectivity analyses of the human brain: limitations and improvement. *J Neuroimaging* 24:176–186.

Address correspondence to:

Xiaobo Li

Department of Biomedical Engineering

New Jersey Institute of Technology

323 Martin Luther King Boulevard, Fenster 613

Newark, NJ 07102

E-mail: xli.aecom@gmail.com; xiaobo.li@njit.edu